

# Altered Sodium and Potassium, but not Calcium Currents in Cerebellar Granule Cells in an In Vitro Model of Neuronal Injury

Katarína Ondáčová<sup>1</sup> · Dana Jurkovičová<sup>2</sup> · Eubica Lacinová<sup>1</sup> 

Received: 21 June 2016 / Accepted: 8 August 2016 / Published online: 12 August 2016  
© Springer Science+Business Media New York 2016

**Abstract** Acute injury of central nervous system (CNS) starts a cascade of morphological, molecular, and functional changes including formation of a fibrotic scar, expression of transforming growth factor beta 1 (TGF- $\beta$ 1), and expression of extracellular matrix proteins leading to arrested neurite outgrowth and failed regeneration. We assessed alteration of electrophysiological properties of cerebellar granule cells (CGCs) in two in vitro models of neuronal injury: (i) model of fibrotic scar created from coculture of meningeal fibroblasts and cerebral astrocytes with addition of TGF- $\beta$ 1; (ii) a simplified model based on administration of TGF- $\beta$ 1 to CGCs culture. Both models reproduced suppression of neurite outgrowth caused by neuronal injury, which was equally restored by chondroitinase ABC (ChABC), a key disruptor of fibrotic scar formation. Voltage-dependent calcium current was not affected in either injury model. However, intracellular calcium concentration could be altered as an expression of inositol trisphosphate receptor type 1 was suppressed by TGF- $\beta$ 1 and restored by ChABC. Voltage-dependent sodium current was significantly suppressed in CGCs cultured on a model of fibrotic scar and was only partly restored by ChABC. Administration of TGF- $\beta$ 1 significantly shifted current–voltage relation of sodium current toward more positive membrane potential without change to maximal current amplitude. Both transient and sustained

potassium currents were significantly suppressed on a fibrotic scar and restored by ChABC to their control amplitudes. In contrast, TGF- $\beta$ 1 itself significantly upregulated transient and did not change sustained potassium current. Observed changes of voltage-dependent ion currents may contribute to known morphological and functional changes in injured CNS.

**Keywords** Cerebellar granule cells · TGF- $\beta$ 1 · Fibrotic scar · Chondroitinase ABC · Sodium current · Potassium current · Calcium current

## Introduction

Traumatic injury of central nervous system (CNS) is accompanied by a formation of scarring tissue in the lesion site, either glial scar or a fibrotic scar (Berry et al. 1983; Carbonell and Boya 1988; Fawcett and Asher 1999). Fibrotic scar both protects surrounding tissue from further infection and hinders axonal regeneration on the site of damage (Shearer and Fawcett 2001; Shearer et al. 2003). Creation of a fibrotic scar is a complex process including aggregation of fibroblasts, formation of glia limitans, deposition of extracellular matrix molecules (ECMs), as well as enhanced expression of molecules inhibiting axonal growth like chondroitin sulfate proteoglycans (CSPGs), phosphacan, ephrin-B2, NG2 proteoglycan, Versican, and Semaphorin 3A and 3B (Kawano et al. 2012). Elimination of the fibrotic scar is necessary for axonal regeneration in the CNS lesion site. Lesion site develops not only after traumatic injury but also after disruption of the blood–brain barrier or inflammation in various neuronal disorders such as a stroke, spinal cord injury, and multiple sclerosis (Fernandez-Klett and Priller 2014). Therefore,

✉ Eubica Lacinová  
lubica.lacinova@savba.sk

<sup>1</sup> Institute of Molecular Physiology and Genetics, Slovak Academy of Sciences, Dubravská cesta 9, 84005 Bratislava, Slovakia

<sup>2</sup> KR D molecular technologies s. r. o, Saratovská 26, 84201 Bratislava, Slovakia

understanding the process of scar formation and its elimination is a prerequisite for a design of efficient therapeutic strategies. Accordingly, *in vitro* fibrotic scar models can offer a unique experimental and practical approach for investigation of underlying mechanisms on the single cell level.

In the past, several research groups have tried to employ different *in vitro* models of CNS injury or fibrotic scar. Initially, coculture of cerebral astrocytes and meningeal fibroblasts was used as an *in vitro* model of CNS lesion (Struckhoff 1995; Shearer et al. 2003; Wanner et al. 2008). More recently, Kimura-Kuroda and coauthors have developed more advanced model of the fibrotic scar by administration of transforming growth factor beta 1 (TGF- $\beta$ 1) to the coculture of cerebral astrocytes and meningeal fibroblasts (Kimura-Kuroda et al. 2010). In contrast to simple coculture model, this model more accurately reproduced morphological, molecular, and functional characteristics of injured CNS, including aggregation of fibroblasts, deposition of ECMs, enhanced expression of chondroitin sulfate, NG2, semaphorin 3A and tenascin-C, formation of glia limitans, and inhibition of axon growth (Kimura-Kuroda et al. 2010).

CNS injury upregulates the expression of anti-inflammatory cytokine TGF- $\beta$ 1 around the lesion site (Komuta et al. 2010). TGF- $\beta$ 1 is one of the most important factors involved in formation of the fibrotic scar. In rat brain, this process was promoted by TGF- $\beta$ 1 administration and prevented by its neutralization with TGF- $\beta$ 1 antibody (Logan et al. 1994).

Similarly, upregulation of CSPGs in the injury site is considered to be the major factor preventing axonal regeneration (Carulli et al. 2005; Kawano et al. 2012). An application of chondroitinase ABC (ChABC), a chondroitin sulfate-degrading enzyme, into the lesion site completely suppressed the fibrotic scar formation, reduced the glial scar, and promoted axonal regeneration of central neurons (Li et al. 2007, 2013).

Until now, *in vitro* models of neural injury were preferentially used for investigation and description of morphological and molecular characteristics. To our best knowledge, we have not found any data published on voltage-dependent sodium, potassium, and calcium currents and their changes in relation to an *in vitro* neuronal injury model. The expression of voltage-dependent sodium, potassium, and calcium channels represent an important functional feature of neurons. These channels participate not only on electrical signaling but also contribute to regulation of neurite outgrowth. Deregulated intracellular calcium concentration is a well-established regulator of neuronal development and plasticity (Jaskova et al. 2012; Mattson 2007). Stimulation of voltage-gated sodium channels (George et al. 2009; Jabba et al. 2010) or

inhibition of voltage-dependent potassium channels (Cao et al. 2014) facilitated neurite outgrowth in cerebrocortical neurons.

In our experiments, we used the Kimura-Kuroda's model of fibrotic scar (Kimura-Kuroda et al. 2010), and we focused on recognition and definition of electrophysiological parameters of the employed neuronal cells. We analyzed possible alterations of voltage-dependent calcium, sodium, and potassium currents in cerebellar granule cells (CGCs) cultured on *in vitro* fibrotic scar model and consequently, the effect of administration of ChABC preventing these alterations. In parallel, we tested whether individual administration of TGF- $\beta$ 1 to CGCs may trigger similar changes, and whether ChABC administration may have any effect under these conditions.

## Materials and Methods

Wistar rats purchased from the Institute of Experimental Pharmacology and Toxicology, Slovak Academy of Sciences, Department of Toxicology and Animal breeding, Dobrá voda, Slovakia were used in all experiments. Animal handling protocols were approved by the institutional Committee for ethical handling of animals and State Veterinary and by the State Veterinary and Food Administration of the Slovak Republic in accordance with European laws and policies of animal welfare. All efforts were made to minimize the number of animals used and their suffering.

### Primary Culture of Fibroblasts and Astrocytes

Meninges and cerebral cortices of 1- to 2-day-old Wistar rats were extracted, transferred to sterile phosphate-buffered saline, and homogenized by trituration. Meningeal fibroblasts and cerebral astrocytes were cultivated separately in 25 cm<sup>2</sup> culture flasks in Basal Medium Eagle (BME) with Earlé's salts (Sigma-Aldrich, Slovakia) supplemented with heat-inactivated calf fetal serum (10 %), L-Glutamine (2 mM, Lonza, Verviers, Belgium), and gentamicin sulfate (100  $\mu$ g/ml, Lonza, Verviers, Belgium). Fully confluent cells were released by trypsin, resuspended in a fresh media, and further cultivated over a period of 2–12 weeks. During this period, fibroblasts and astrocytes were used for a formation of *in vitro* fibrotic scar model.

### In Vitro Model of the Fibrotic Scar

An *in vitro* model of the fibrotic scar was adopted from Kimura-Kuroda and coauthors (Kimura-Kuroda et al. 2010). Briefly, fibroblasts and astrocytes were seeded on

opposite site of poly-L-lysine (PLL-10  $\mu\text{g}/1\text{ ml}$ , Sigma-Aldrich, Slovakia)-coated coverslips in 24-well plate at a density of  $2 \times 10^4$  cells per a 12 mm coverslip. Cells were cultivated in BME with additives as described above and formed separate flat colonies which rarely overlapped. Cell clustering occurred at the astrocyte/fibroblast border within 7 days. At that time, TGF- $\beta$ 1 (10 ng/ml, #C63504; PromoKine, Heidelberg, Germany) was added to the cell culture media and a fibrotic scar-like formation developed within 7 following days.

### Cerebellar Granule Cells Cultured for an Assessment of the TGF- $\beta$ 1 Effect

Cerebellar cortices from 6-day old Wistar rats were minced, trypsinized, and triturated in BME with KCl (25 mM). Cerebellar granule cells (CGC) were seeded on PLL-coated coverslips in the density of  $7 \times 10^5$  cells per 12 mm coverslip. Cells were cultivated in BME with Earlé's salts (Sigma-Aldrich, Germany) supplemented with heat-inactivated calf fetal serum (10 %), L-Glutamine (2 mM, Lonza, Verviers, Belgium), gentamicin sulfate (100  $\mu\text{g}/\text{ml}$ , Lonza, Verviers, Belgium), and KCl (25 mM). 24 h after plating cells were supplemented with cytosine  $\beta$ -D-arabinofuranoside (10  $\mu\text{M}$ ; Sigma-Aldrich, Germany) to inhibit proliferation of non-neuronal cells. After 6 days of cultivation in vitro (DIV6) cells were divided into three groups: (i) control cells; (ii) cells cultured in the presence of TGF- $\beta$ 1 (10 ng/ml); and (iii) cells cultured in the presence of TGF- $\beta$ 1 (10 ng/ml) and ChABC (0.5 U/ml) and corresponding substances were added to the culture medium. On DIV9 morphological and electrophysiological analyses were initiated. In all cases, cells were incubated at 37 °C in a humidified 5 %  $\text{CO}_2$ , 20 %  $\text{O}_2$ , and 75 %  $\text{N}_2$  atmosphere.

### Primary Culture of Cerebellar Granule Cells on an In Vitro Fibrotic Scar Model

CGCs were prepared as described above. Three hours before seeding of CGCs, in one half of wells containing prepared fibrotic scar model growing in media with TGF- $\beta$ 1, culture medium was exchanged for TGF- $\beta$ 1-free medium supplemented with ChABC (0.5 U/ml; #C3667; Sigma-Aldrich, Germany) (Li et al. 2013). In the other half of the wells containing fibrotic scar model, the medium was left unchanged. After 3 hours of incubation, just before seeding of CGCs, culture medium was removed from all wells. Dissociated cerebellar granule cells (CGCs) in BME medium with KCl (25 mM) (TGF- $\beta$ 1-free) were divided into three groups and seeded (i) on a model of fibrotic scar, (ii) on a model of fibrotic scar with ChABC (0.5 U/ml) added, and (iii) on PLL-coated coverslips. CGCs were

seeded equally at density of  $7 \times 10^5$  cells per 12 mm coverslip. All three groups were cultivated in BME with additives as described above. After 3 days of cultivation, morphological and electrophysiological analyses were performed. Plates containing partly damaged cells were excluded from further analyses.

### Expression of IP<sub>3</sub> Receptor Type 1

Total RNA was isolated from CGCs homogenized in TRI reagent (#K1622; Thermo Scientific, Waltham, Massachusetts, USA). Reverse transcription was performed with 1.5 mg of total RNA using the RevertAid First Strand cDNA Synthesis Kit (#K1622, Thermo Scientific) with pd(N6) primer. Afterwards, conventional PCR was performed using specific oligonucleotides for IP<sub>3</sub>R1 (Jurkovicova et al. 2007). The expression of housekeeper gene glyceraldehyde 3-phosphate dehydrogenase (GAPDH) was evaluated for relative comparison. PCR program, primers, and methods of evaluation of individual bands are described in detail in (Jurkovicova et al. 2007). Approximately  $15 \times 10^6$  pelleted cells were used for each analysis.

### Electrophysiological Recordings

Current through sodium ( $I_{\text{Na}}$ ), calcium ( $I_{\text{Ca}}$ ), and potassium ( $I_{\text{K}}$ ) channels were measured in the whole-cell patch clamp configuration using the HEKA EPC10 amplifier (HEKA Electronics, Lambrecht, Germany). The extracellular solution for  $I_{\text{K}}$  contained (in mM): 115 NaCl; 4 KCl; 10 HEPES; 2  $\text{CaCl}_2$ ; 1  $\text{MgCl}_2$ ; 30 D-glucose at a pH 7.4 (with NaOH). 1  $\mu\text{M}$  Tetrodotoxine (TTX; Abcam, Cambridge, UK) was added to the extracellular solution to block  $I_{\text{Na}}$ . The intracellular solution contained (in mM): 120  $\kappa$ -gluconate; 20 KCl; 2  $\text{MgCl}_2$ ; 2  $\text{Na}_2\text{ATP}$ ; 0.25  $\text{Na}_2\text{GTP}$ ; 10 HEPES at a pH 7.3 (with KOH). Currents through sodium and calcium channels were measured using an intracellular solution containing (in mM): 135 CsCl; 3  $\text{Na}_2\text{-ATP}$ ; 20 TEA-Cl; 3 EGTA; 10 HEPES; 0.4  $\text{Na}_2\text{-GTP}$ ; 2  $\text{MgCl}_2$  at a pH 7.4 (with CsOH). Barium was used as a charge carrier for measurements of the current through the calcium channels. The extracellular solution contained (in mM): 115 NaCl, 10  $\text{BaCl}_2$ , 3 CsCl, 10 HEPES, 2  $\text{CaCl}_2$ , 0.5 mM  $\text{MgCl}_2$  at a pH 7.4 (with NaOH). Bath solution for measurement of  $I_{\text{Ca}}$  additionally contained 1  $\mu\text{M}$  TTX to block  $I_{\text{Na}}$ . Osmolarity of an intracellular solution was approximately 290–300 mOsmol/l (measured by Osmomat 030-Gonotec, Germany). Osmolarity of an extracellular solution was adjusted by adding glucose so that a final osmolarity was 2–3 mOsm/l lower than the osmolarity of corresponding intracellular solution.

Potassium currents were activated from a holding potential of  $-80\text{ mV}$  by 400 ms long depolarizing pulses

with amplitudes ranging from  $-70$  to  $+80$  mV. Currents through calcium channels were elicited by a series of 150 ms long depolarizing pulses from a holding potential of  $-80$  mV to a voltages between  $-70$  and  $+70$  mV. Sodium currents were activated from a holding membrane potential of  $-100$  mV by 5 ms long depolarizing voltage pulses to the voltages ranging from  $-80$  to  $+60$  mV.

## Analysis

### Neurite Length Measurement

Neurite length was analyzed from microscopic pictures using ImageJ software. The length of the ruler was calibrated in micrometers using the scale tool of the microscope camera and statistically evaluated by GraphPad InStat 3 software. Only neuronal processes longer than the cell body diameter were evaluated. Results are presented as mean  $\pm$  SEM from 5 independent preparations of CGCs. Lengths of 25–30 neurites were averaged in each preparation.

### Electrophysiology Data

Whole-cell current densities were calculated by dividing peak current amplitude by cell capacitance. Data were recorded by HEKA Patchmaster v2  $\times$  73.3 (HEKA Electronics; Lambrecht/Pfalz, Germany) and analyzed by HEKA Fitmaster v2  $\times$  73.3 and Origin 8.1 (OriginLab Co., Northampton, MA, USA). Current–voltage relations for  $I_{Na}$  were fitted by the combined Boltzmann–Ohm equation:

$$I(V) = (V - V_R) \frac{g_{\max}}{1 + e^{-\frac{-(V-V_{0.5})}{dV}}},$$

where  $I(V)$  is the amplitude of the current activated by the depolarizing pulse to the membrane voltage  $V$ ,  $V_R$  is the reversal potential,  $g_{\max}$  is the maximal slope conductance,  $V_{0.5}$  is the half-maximal activation voltage, and  $dV$  is the activation slope factor (Karmazinova and Lacinova 2010).

### Statistical Analysis

Results are presented as a mean  $\pm$  standard error of mean (SEM). Statistical differences between three groups were determined by One-Way Analysis of Variance (ANOVA) followed by Tukey test for pairwise multiple comparisons. Two datasets were compared by unpaired  $t$  test. Probability  $p < 0.05$  was considered significant (GraphPad InStat 3).

## Results

In our experiments, we compared morphological and electrophysiological properties of cerebellar granule cells on two in vitro models of neuronal injury. First, we used an in vitro model of fibrotic scar prepared by coculture of meningeal fibroblasts and cerebral astrocytes in the presence of TGF- $\beta$ 1 in culture media (Kimura-Kuroda et al. 2010). We compared (i) CGCs cultured on a fibrotic scar model, (ii) CGCs cultured on a fibrotic scar model with ChABC administered, and (iii) CGCs cultured in a dish with culture medium (control conditions, without fibrotic scar). CGCs were allowed to grow for 3 days. On Day 3 in vitro (DIV3) CGCs properties were analyzed. In second model, we evaluated the effect of TGF- $\beta$ 1. CGCs were seeded on culture dishes in a control medium and were allowed to grow for 6 days. On DIV6, all dishes were divided into three equal groups: control, TGF- $\beta$ 1-administered, and TGF- $\beta$ 1 + ChABC administered. On DIV9, morphological and electrophysiological properties of CGCs were analyzed.

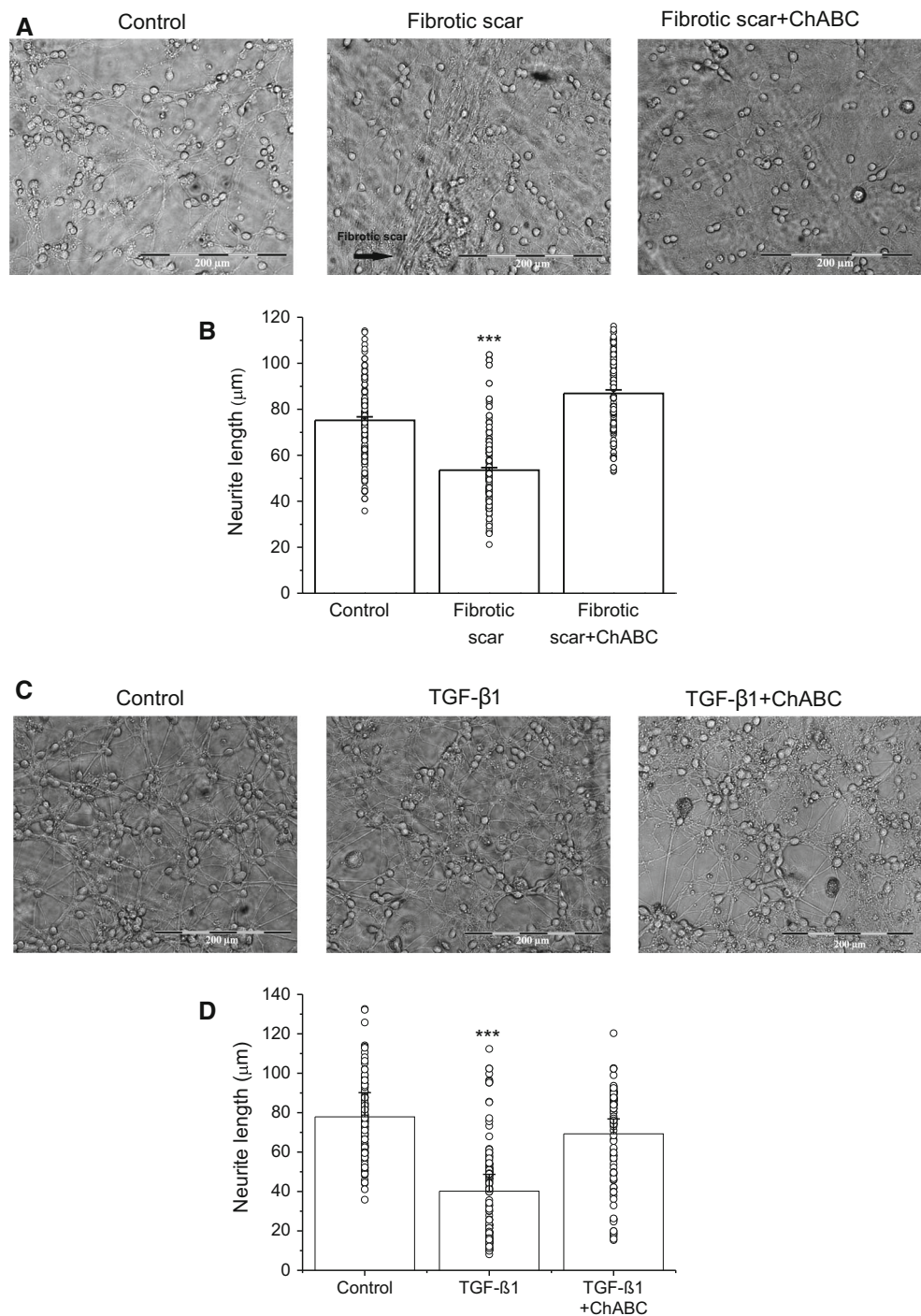
### Neurite Outgrowth in In Vitro Models of Neuronal Injury

Neurite outgrowth may be considered as one of the indicators of cells health. Neurite outgrowth of primary CGCs cultured on fibrotic scar or in its close proximity (Fig. 1a) was significantly suppressed at the DIV3. Average neurite length of CGCs cultured under the control conditions was  $75.2 \pm 1.5$   $\mu$ m while the average neurite length of CGCs cultured on the fibrotic scar was  $53.5 \pm 1.1$   $\mu$ m ( $p < 0.001$ ). ChABC restored the neurite outgrowth on fibrotic scar to the average neurite length  $86.9 \pm 1.5$   $\mu$ m (Fig. 1b).

An exposure to TGF- $\beta$ 1 suppressed the neurite outgrowth of CGCs to a bigger extent than the conditions on a fibrotic scar model ( $77.9 \pm 12.3$   $\mu$ m in control conditions;  $40.2 \pm 8.5$   $\mu$ m in the presence of TGF- $\beta$ 1;  $p < 0.001$ , Fig. 1c, d). Growth suppression was prevented by simultaneous administration of ChABC ( $69.3 \pm 7.5$   $\mu$ m in ChABC).

Changes in neuron length were not caused by an alteration of cell density, as this was not significantly different upon any experimental conditions (Fig. 1a: control,  $108 \pm 14$  cells; fibrotic scar,  $111 \pm 4$  cells; ChABC,  $119 \pm 12$  cells per each field; Fig. 1c: control,  $90 \pm 4$  cells; TGF- $\beta$ 1,  $94 \pm 3$  cells; TGF- $\beta$ 1 + ChABC,  $89 \pm 5$  per field). Eight visual fields were evaluated under each condition.

**Fig. 1** Altered CGCs neurite length in in vitro models of neuronal injury. **a** Examples of CGCs cultured under the control conditions (*left panel*), on an in vitro model of fibrotic scar (*middle panel*), and on an in vitro model of fibrotic scar with ChABC added (*right panel*). In the *middle panel*, formed scar is visible. It disappeared in the presence of ChABC. Scale bar represents 200  $\mu\text{m}$ . **b** An average length of neurite cultured under the control conditions ( $n = 5$  preparations, 30 neurons per preparation), on an in vitro model of fibrotic scar ( $n = 5$  preparations, 30/29/29/30/30 neurons in individual preparations), and on an in vitro model of fibrotic scar with ChABC added ( $n = 5$  preparations, 27/29/25/30/30 neurons in individual preparations), as marked.  $***p < 0.001$ ;  $F = 157.2$ . **c** Examples of CGCs cultured under the control conditions (*left panel*), in the presence of TGF- $\beta 1$  (*middle panel*), and in the presence of TGF- $\beta 1$  with ChABC (*right panel*). Scale bar represents 200  $\mu\text{m}$ . **d** An average length of neurite cultured under the control conditions ( $n = 5$  preparations, 30/30/29/29/29 neurons in individual preparations), in the presence of TGF- $\beta 1$  ( $n = 5$  preparations, 25/30/29/26/27 neurons in individual preparations), and the presence of TGF- $\beta 1$  with ChABC ( $n = 3$  preparations, 30 neurons in each preparation), as marked.  $***p < 0.001$ ,  $F = 69.2$



### Voltage-Gated Ion Currents in In Vitro Models of Neuronal Injury

Voltage-dependent calcium, sodium, and potassium currents represent key components of neuronal excitability. Therefore, we further analyzed alteration of these three types of ionic currents in both the models of neuronal injury.

Sodium channels carry inward flow of  $\text{Na}^+$  ions through plasma membrane and generate sodium current ( $I_{\text{Na}}$ ),

which participates in rising phase of action potentials (APs). Additionally,  $\beta$  subunit of voltage-dependent sodium channels promotes neurite outgrowth (Davis et al. 2004). Part of cultured CGCs developed measurable sodium current on the DIV3 (percentage of all tested cells with measurable  $I_{\text{Na}}$ : control, 30 % (10/33); fibrotic scar, 29 % (14/48); fibrotic scar + ChABC; 30 % (18/61)). Amplitudes of  $I_{\text{Na}}$  in CGCs grown on fibrotic scar were significantly lower compared to control CGCs at

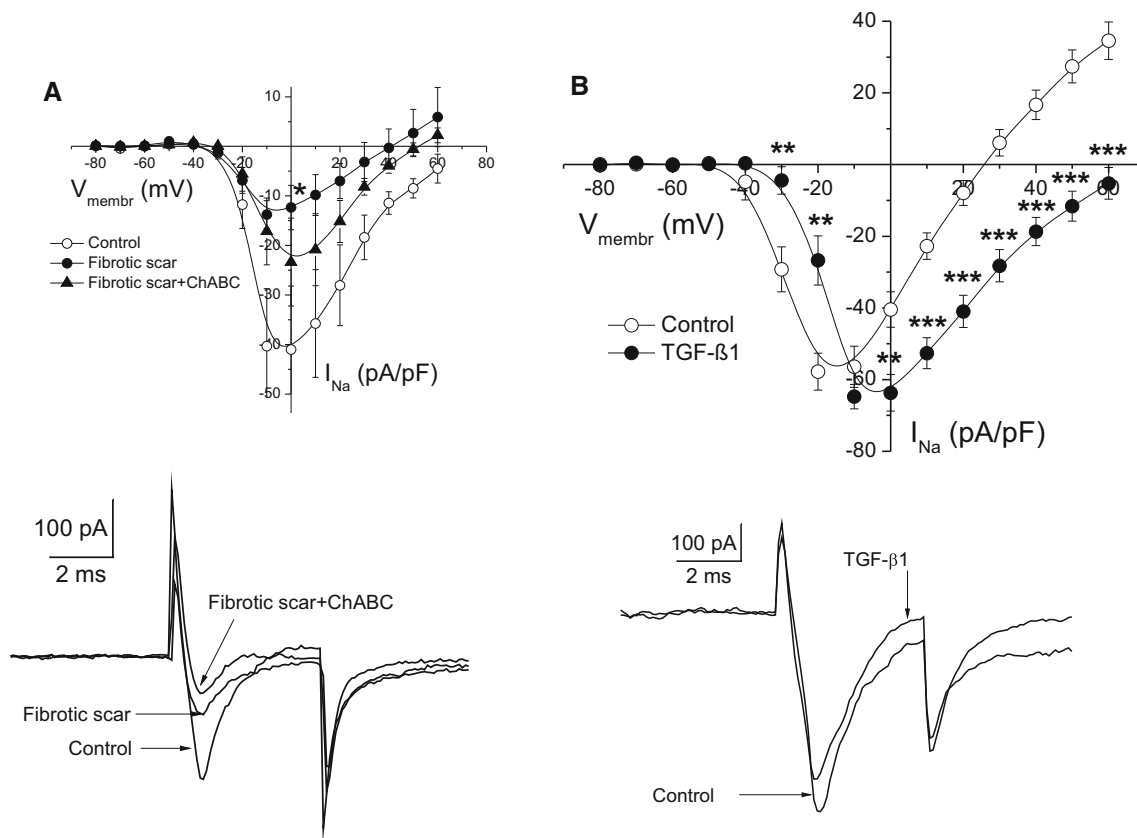


**Fig. 2** Sodium currents measured in both in vitro models of neuronal injury. **a**  $I$ - $V$  relations for  $I_{Na}$  measured from CGCs cultured under the control conditions (open circle,  $n = 10$ ), on an in vitro model of fibrotic scar (closed circle,  $n = 11$ ), and on an in vitro model of fibrotic scar with ChABC added (closed triangle,  $n = 11$ ).  $*p < 0.05$ ;  $F = 5.2$ . Examples of current traces measured by depolarization pulse

to 0 mV are shown below the graph. **b**  $I$ - $V$  relations for  $I_{Na}$  measured from CGCs cultured under the control conditions (open circle,  $n = 14$ ), and after 72 h exposure to TGF- $\beta 1$  (closed circle,  $n = 14$ ).  $**p < 0.01$ ,  $***p < 0.001$  compared to the control. Examples of current traces measured by depolarization pulse to 0 mV are shown below the graph

**Table 1** Experimental data presented in Fig. 2a were fitted by the combined Boltzmann–Ohm equation

	$V_{0.5}$ (mV)	$g_{max}$ (pS/pF)	$n$
Control	$-13.9 \pm 2.7$	$1.33 \pm 0.24$	10
Fibrotic scar	$-14.4 \pm 1.1$	$0.43 \pm 0.07^{***}$	11
Fibrotic scar + ChABC	$-7.2 \pm 2.1^{\#}$	$0.78 \pm 0.35^*$	11

Resulting values for half-maximal activation voltage ( $V_{0.5}$ ) and a maximal slope conductance  $g_{max}$  as well as the number of tested cells ( $n$ ) are shown

$*** p < 0.001$ ; control versus fibrotic scar;  $* p < 0.05$ ;  $F = 3.2$  control versus fibrotic scar + ChABC;  $\# p < 0.05$ ;  $F = 4.8$  fibrotic scar versus fibrotic scar + ChABC

depolarizations greater or equal to  $-10$  mV (Fig. 2a). Inhibition of fibrotic scar formation by ChABC did not fully recover  $I_{Na}$  to the control level, nevertheless, the current amplitude was no more significantly lower than the current amplitude measured under the control conditions (Fig. 2a). Fitting of individual  $I$ - $V$  relations with a

**Table 2** Experimental data presented in Fig. 2b were fitted by the combined Boltzmann–Ohm equation

	$V_{0.5}$ (mV)	$g_{max}$ (pS/pF)	$n$
Control	$-27.3 \pm 1.4$	$1.60 \pm 0.18$	14
TGF- $\beta 1$	$-18.2 \pm 1.6^{***}$	$1.35 \pm 0.14$	14

Resulting values for half-maximal activation voltage ( $V_{0.5}$ ) and a maximal slope conductance  $g_{max}$  as well as the number of tested cells ( $n$ ) are shown

$*** p < 0.001$ ; control versus TGF- $\beta 1$

Boltzmann–Ohm equation (Table 1) showed significant decrease of the maximal slope conductance for CGCs cultured either on a fibrotic scar or on a fibrotic scar with ChABC. Additionally, voltage dependence of  $I_{Na}$  activation was significantly shifted to more depolarized membrane voltages when cells were cultured on a fibrotic scar in the presence of ChABC (Table 1). In contrast, 72 h of TGF- $\beta 1$  exposure of CGCs after 6 days in vitro did not alter peak value of  $I_{Na}$   $I$ - $V$  relation but shifted the peak

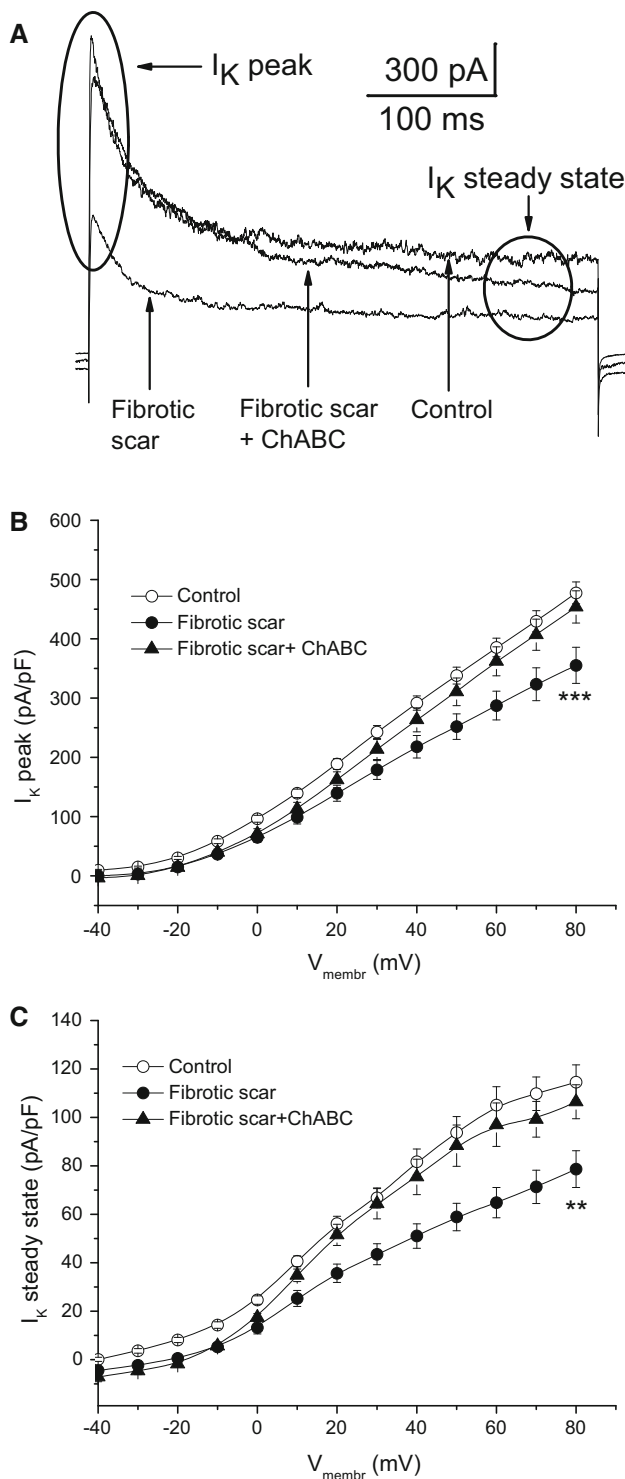


**Fig. 3** Potassium currents measured on an in vitro fibrotic scar model. **a** Representative examples of potassium currents measured from CGCs seeded in control conditions, on an in vitro fibrotic scar model, and on an in vitro fibrotic scar model with ChABC added, as marked. *Arrows* indicate at which time point a peak current amplitude and a steady-state current amplitude were measured. **b**  $I$ - $V$  relations for a peak current amplitudes measured from CGCs cultured under the control conditions (*open circle*,  $n = 21$ ), on an in vitro model of fibrotic scar (*closed circle*,  $n = 18$ ), and on an in vitro model of fibrotic scar with ChABC added (*closed triangle*,  $n = 19$ ).  $***p < 0.001$ ;  $F = 16.6$  at  $+80$  mV. **c**  $I$ - $V$  relations for a steady-state current amplitudes evaluated from the same CGCs as in the panel **b**.  $**p < 0.01$ ;  $F = 7.6$  at  $+80$  mV

value significantly toward more depolarized membrane potentials (Fig. 2b, Table 2). On DIV9, all tested cells expressed sodium channels in a sufficient density.

Voltage-gated potassium channels are the key determinants of membrane excitability. Multiple types of voltage-dependent potassium currents including transient inactivating A-type current ( $I_A$ ) and non-inactivating delayed rectifier current are present in CGCs. Therefore, we analyzed both peak amplitude and steady-state component of potassium currents (Fig. 3a). In a group of CGCs seeded on a fibrotic scar, we observed significant decrease in a maximal peak amplitude of  $I_A$  (at the membrane potential of  $+80$  mV: control,  $478 \pm 18$  pA/pF,  $n = 21$ ; fibrotic scar,  $355 \pm 31$  pA/pF,  $n = 18$ ;  $p < 0.001$ ). The presence of ChABC recovered peak amplitude of  $I_A$  back to the control level (at the membrane potential of  $+80$  mV: fibrotic scar plus ChABC,  $454 \pm 27$  pA/pF,  $n = 19$ ; Fig. 3b). Steady-state amplitude (Fig. 3c) decreased to a similar extent (at a membrane potential of  $+80$  mV: control,  $115 \pm 7$  pA/pF,  $n = 21$ ; fibrotic scar,  $79 \pm 8$  pA/pF,  $n = 18$ ;  $p < 0.01$ ). Again, exposure to ChABC prevented this decrease (at a membrane potential of  $+80$  mV: fibrotic scar plus ChABC,  $107 \pm 7$  pA/pF,  $n = 19$ ).

After 72 h of TGF- $\beta$ 1 exposure of CGCs, we observed significant increase in the maximal peak amplitude of  $I_K$  at a membrane potential  $+80$  mV compare to control group of neurons (at a membrane potential of  $+80$  mV: control,  $627 \pm 85$  pA/pF,  $n = 15$ ; TGF- $\beta$ 1,  $831 \pm 61$  pA/pF  $n = 14$ ;  $p < 0.05$ ; Fig. 4a, b). Steady-state current amplitude was not significantly affected (Fig. 4a, c).

Calcium currents ( $I_{Ca}$ ) contribute to both neuronal excitability and a neuronal development.  $I$ - $V$  relations for

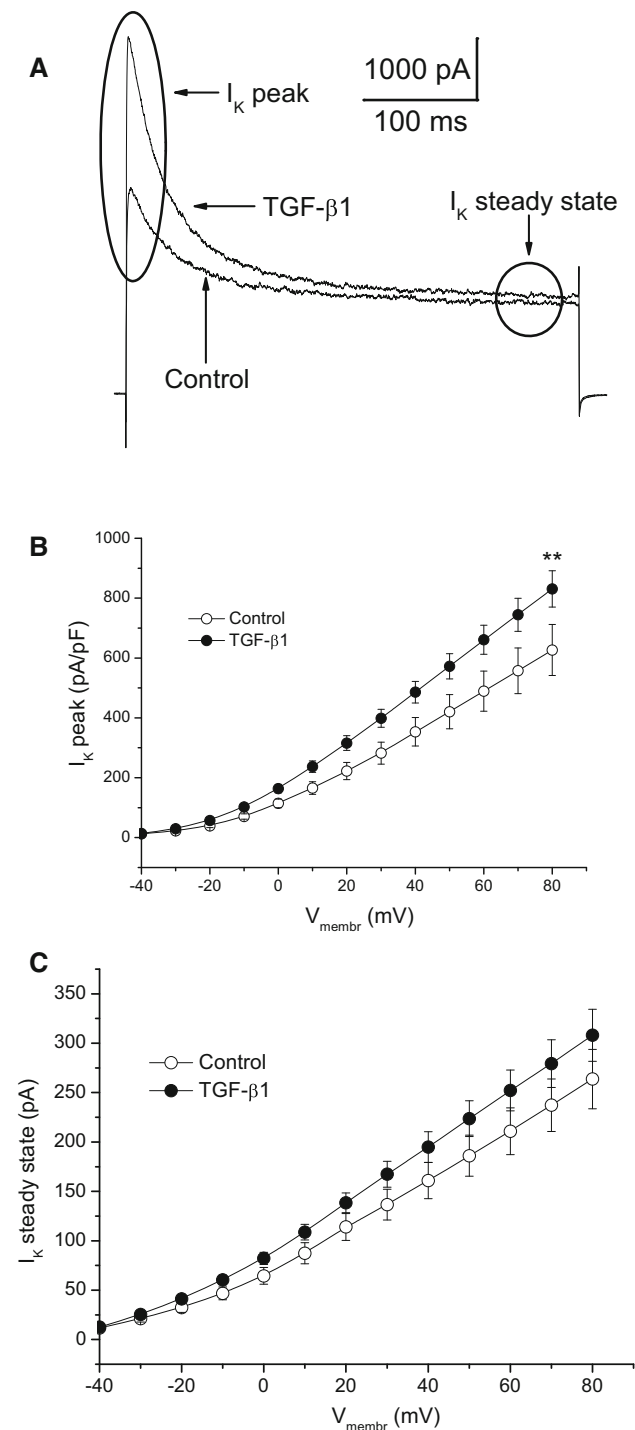


**Fig. 4** Potassium currents measured after a TGF- $\beta$ 1 treatment. **a** Representative examples of potassium currents measured from CGCs cultured under the control conditions, and CGCs to which TGF- $\beta$ 1 was added for 72 h, as marked. Peak current amplitude and a steady-state current amplitude were measured at a time point indicated by an arrow. **b**  $I$ - $V$  relations for a peak current amplitudes measured from CGCs cultured under the control conditions (open circle,  $n = 15$ ), and in the presence of TGF- $\beta$ 1 (closed circle,  $n = 14$ ).  $**p < 0.01$ ;  $F = 5.9$  **c**  $I$ - $V$  relations for a steady-state current amplitude evaluated from the same CGCs as in the *panel* (b)

$I_{Ca}$  measured with the  $Ba^{2+}$  as a charge carrier from CGCs cultured under control conditions were not significantly different from those measured from CGCs cultured on a fibrotic scar and/or from those cultured on a fibrotic scar with administered ChABC (Fig. 5a). The percentage of recorded cells with measurable  $I_{Ca}$  decreased from 52 % (11/21) of cells cultured under the control conditions to 40 % (11/27) of cells cultured on a fibrotic scar. When ChABC was added to a fibrotic scar model, percentage of cells with measurable  $I_{Ca}$  increased back to 46 % (12/26). Similar to a lack of the effect of fibrotic scar on  $I_{Ca}$  amplitude, exposure of CGCs to TGF- $\beta$ 1 did not alter maximal peak amplitude of  $I_{Ca}$  (Fig. 5b).

### Modulation of $IP_3R1$ by TGF- $\beta$ 1

Lack of an effect on voltage-dependent calcium current was surprising, as previously we have demonstrated altered expression of multiple calcium transporters ( $IP_3R1$ ,  $IP_3R2$ , RyR1, RyR2, and SERCA2) in CGCs in the presence of TGF- $\beta$ 1 (Jaskova et al. 2014). Major role in TGF- $\beta$ 1 effects on CGCs had a suppressed expression of  $IP_3R1$  (Jaskova et al. 2014). Therefore, we tested whether the ChABC may restore also  $IP_3R1$  expression. Indeed, decrease of mRNA expression of  $IP_3R1$  was fully prevented by the presence of ChABC (Fig. 6) that fully correlated with ChABC-restored neurite outgrowth.

### Discussion

Traumatic nerve injury is a complex status accompanied by multiple morphological and functional changes including alterations of neuronal excitability (Viviani et al. 2007; Nichols et al. 2015). Changes in morphology and/or expression of various proteins around the site of injury are intensively studied. Less is known about possible changes in membrane excitability on a single neuron level. To define and better understand electrophysiological parameters of neuronal cells cultured on in vitro fibrotic scar model, we have compared two in vitro models of neuronal injury: i) an in vitro fibrotic scar model prepared according to Kimura-Kuroda and coauthors (Kimura-Kuroda et al. 2010) and ii) a simplified model based on administration of the fibrotic scar inducer TGF- $\beta$ 1 to a primary CGCs culture. Suppressed neurite outgrowth can be considered as a signature of nerve injury (Anderson et al. 2016). Both the models effectively reproduced this feature verifying our experimental conditions. In both cases ChABC fully restored the neurite outgrowth. This result confirmed previous reports demonstrating an ability of ChABC to



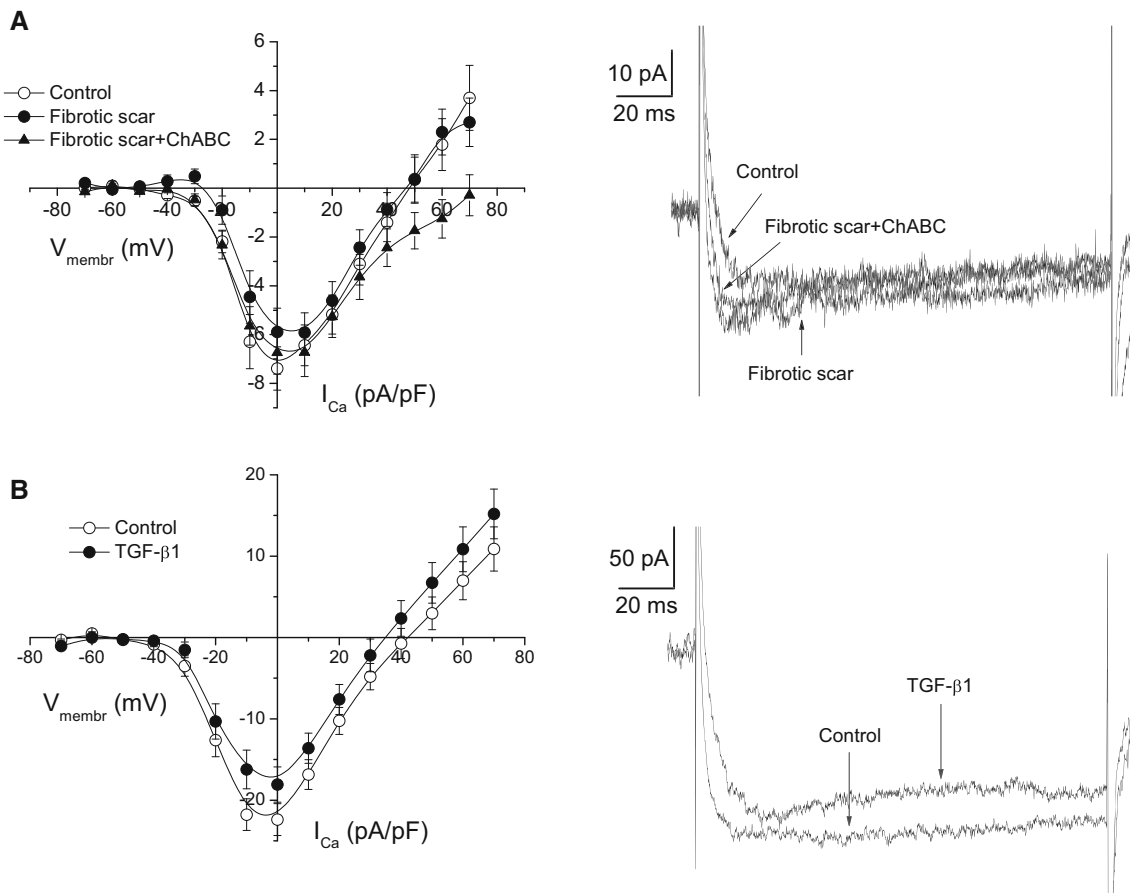


**Fig. 5** Calcium currents measured in both in vitro models of neuronal injury. **a**  $I$ - $V$  relations for  $I_{\text{Ca}}$  measured from CGCs cultured under the control conditions (open circle,  $n = 10$ ), on an in vitro model of fibrotic scar (closed circle,  $n = 10$ ), and on an in vitro model of fibrotic scar with ChABC added (closed triangle,  $n = 11$ ). Examples of current traces measured by depolarization pulse to 0 mV

are shown on the right. **b**  $I$ - $V$  relations for  $I_{\text{Ca}}$  measured from CGCs cultured under the control conditions (open circle,  $n = 14$ ), and after 72 h exposure to TGF- $\beta$ 1 (closed circle,  $n = 18$ ). Examples of current traces measured by depolarization pulse to 0 mV are shown on the right

suppress fibrotic scar formation and to promote neurite outgrowth (Li et al. 2007, 2013; Morgenstern et al. 2002). Additionally, we observed the same process when TGF- $\beta$ 1 was added to a primary CGCs culture. Therefore we can conclude that, in contrast to suggestion of Susarla and coauthors (Susarla et al. 2011), TGF- $\beta$ 1 ability to induce secretion of CSPGs which impede neuronal growth does not require the presence of astrocytes.

Main focus of our work was on alterations of voltage-dependent ion currents in both the models of neuronal injury. Voltage-dependent sodium current as well as outward potassium current were altered in both neuronal injury models. At least 26 voltage-dependent potassium channel types are expressed in cerebellum. Most abundant  $K_{\text{V}}$  channel subtypes found in CGCs are 1.1, 1.3, 1.5, 2.2, 3.1, 4.2, and 4.3 (Mathie et al. 2003), however, dominant transient inactivating A-type channel is  $K_{\text{V}}4.2$  channel (Heath et al. 2014). Two types of voltage-dependent sodium channels were found in CGCs:  $\text{Na}_{\text{V}}1.2$  and  $\text{Na}_{\text{V}}1.6$

(Schaller and Caldwell 2003). Because of similar kinetics and sensitivity to TTX these channels cannot be distinguished by means of electrophysiology. Substantial role of  $\text{Na}^{+}$  and  $\text{K}^{+}$  channels for normal neuronal development of CGCs was shown. As the A-type current developed, single, and eventually repetitive action potential firing emerged in those cells (Shibata et al. 2000). Further, an amplitude of the A-type  $\text{K}^{+}$  current in these cells increases during development over a similar time course as an amplitude of TTX-dependent  $\text{Na}^{+}$  current (Shibata et al. 2000). It could be expected that pathological conditions will be accompanied by dysregulation of potassium and/or sodium conductance. As  $\text{Na}^{+}$  and  $\text{K}^{+}$  currents are precondition of normal neuronal development their alteration caused by the injury may be an impediment to regeneration process.

We observed sodium current only in part of cells in experiments with a fibrotic scar (DIV3), but virtually in every cell cultured in the presence of TGF- $\beta$ 1 (DIV9). This is in line with previous reports documenting that  $I_{\text{Na}}$

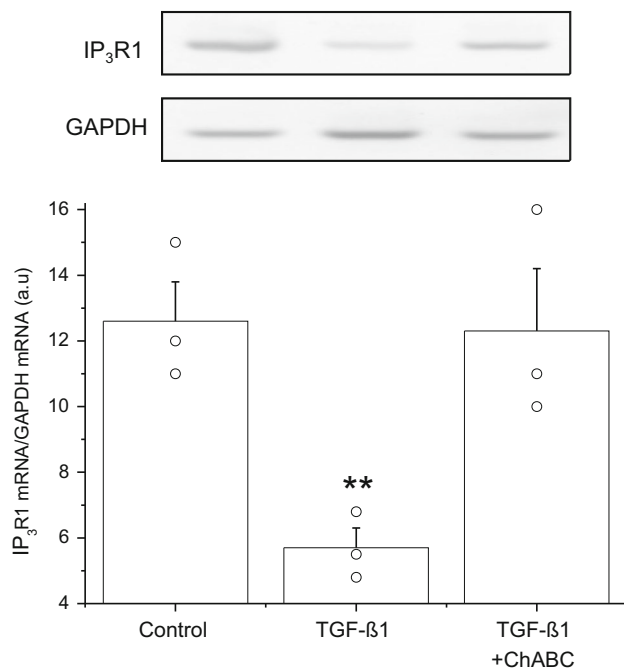


**Fig. 6** Relative comparison of mRNA expression levels for IP<sub>3</sub>R1 evaluated in respect to mRNA expression level for housekeeper gene glyceraldehyde 3-phosphate dehydrogenase (GAPDH) under the control conditions, after 72 h exposure to TGF-β1, and TGF-β1 + ChABC, as marked. For each column number of independent preparations averaged was  $n = 3$ . \*\*  $p < 0.01$ ;  $F = 16.5$  versus control. Representative example of a gel is shown on the top. All PCR products were analyzed on 2 % agarose gels. Optical density (od/mm<sup>2</sup>) of individual bands was measured by Kodak camera and analyzed by PCBAS 2.08e software (Düsseldorf, Germany). Relative quantification was done relatively to housekeeper GAPDH. Positions in a gene for GAPDH (GAPDH1 795–814 and GAPDH2 506–525, overall size 309 bp) and IP<sub>3</sub>R1 (IP<sub>3</sub>R1A 70–90 and, IP<sub>3</sub>R1B 573–593, overall size 535 bp)

gradually appears in cultured CGCs (Stewart et al. 1995). Average amplitude of  $I_{Na}$  as well as its maximal slope conductance decreased significantly when CGCs were cultivated on fibrotic scar and ChABC treatment only partly restored these values to their control level. Simultaneous observation of suppressed neurite outgrowth and decreased  $I_{Na}$  amplitude is in line with reports showing that an enhancement of  $I_{Na}$  enhanced neurite outgrowth in cerebrocortical neurons (Jabba et al. 2010; George et al. 2009).

TGF-β1 itself did not affect maximal  $I_{Na}$  density and a maximal slope conductance but shifted significantly  $I$ – $V$  relation toward more positive membrane potentials. As a result, current amplitudes just above voltage activation threshold were significantly suppressed while they were increased at more positive membrane potentials. This may lead to reduced resurgent sodium current which is required for a neurite outgrowth in CGCs (Brackenbury et al. 2010).

Less prominent decrease in  $I_{Na}$  observed in cells treated with TGF-β1 may be related to reported constitutive

inhibition of sodium channels in CGCs by CaMKII (Carlier et al. 2000). In the presence of TGF-β1 expression of IP<sub>3</sub>R1 and other calcium-transporting proteins (IP<sub>3</sub>R2, RyR1, RyR2, SERCA2) (Jaskova et al. 2014) is suppressed. This may result in decrease in  $[Ca^{2+}]_i$ , which would inhibit activity of  $Ca^{2+}$  binding proteins including CaMKII and relieve the inhibition of  $I_{Na}$ . Expression of calcium-transporting proteins in CGCs cultured on a fibrotic scar model cannot be directly investigated because of mixed cell population. In this model, in addition to enhanced TGF-β1 expression also the expression of multiple extracellular matrix proteins (Kimura-Kuroda et al. 2010) is enhanced. Therefore, alteration of  $[Ca^{2+}]_i$  may differ between CGCs cultured on a fibrotic scar and CGCs cultured in the presence of TGF-β1.

Potassium currents shape the action potential waveform, determine action potential frequency, and contribute to setting the resting membrane potential. Both transient and sustained  $I_K$  were expressed virtually in all cells in our experiments. When CGCs were cultured on a fibrotic scar model, both transient and sustained current were significantly suppressed. The presence of ChABC restored current amplitudes to the control values. This decrease in  $I_K$  is in line with observation of (Ishikawa et al. 1999) that the expression of voltage-gated potassium channels is decreased in dorsal root ganglion neurons following axotomy.

Decreased A-type current can be explained by downregulation of  $K_{V4}$  channels (Heath et al. 2014) and decreased sustained  $K^+$  current by downregulation of  $K_{V2.1}$  channels (Jiao et al. 2007; Zhuang et al. 2012). While an increased expression of TGF-β1 is considered to be one of the major factors affecting pathological processes initiated by neuronal injury and/or inflammation, apparently it is not the cause of suppressed potassium current. We may speculate that signaling pathways activated by TGF-β1 potentiate A-type potassium current amplitude. Significant inhibition of both transient and sustained potassium currents in cells cultured on a fibrotic scar model are caused by other factors. Secreted CSPGs may contribute to this effect because treatment with ChABC restored  $I_K$  to its control amplitude. Underlying mechanism could be a decrease in a gene expression of  $K^+$  channels. Ishikawa and coauthors (Ishikawa et al. 1999) reported a decrease in immunostaining of several subtypes of  $K_V$ s in dorsal root ganglion neurons of axotomized adult rats.

TGF-β1 itself could not mimic this effect. In opposite, transient outward  $I_K$  was significantly enhanced and sustained current was not influenced.

Calcium signaling has essential role in nearly every aspect of neural development (Toth et al. 2016), therefore we found a bit surprising that the amplitude of voltage-dependent calcium current was not altered in either model.

Nevertheless, it is in line with a recent report of Murali and coauthors (Murali et al. 2015) that overall calcium current density is not altered in dorsal root ganglion neurons following neuronal injury. It is well known that the expression of voltage-dependent calcium channels (VDCC) in CGCs is age-dependent both in vivo (Rossi et al. 1994) and in vitro, as no calcium current was detected at the DIV 0.5–5 (Cull-Candy et al. 1989) but it was consistently recorded at DIV 5–13 (Jalonen et al. 1990; Moreira-Lobo et al. 2016; Amico et al. 1995; Ma et al. 2012). We observed calcium current in part of cells in experiments with a fibrotic scar (DIV3), but virtually in every cell cultured in the presence of TGF- $\beta$ 1 (DIV9). We suggest that TGF- $\beta$ 1 may attenuate development of VDCC in CGCs. This attenuation paralleled significant downregulation of IP<sub>3</sub>R1 and other calcium-transporting proteins (IP<sub>3</sub>R2, RyR1, RyR2, and SERCA2) (Jaskova et al. 2014). ChABC restored IP<sub>3</sub>R1 expression in TGF- $\beta$ 1-treated cells and the same time it increased expression of VDCC in CGCs cultured on a fibrotic scar model to the control level. As IP<sub>3</sub>R1 is crucial for CGCs synaptic plasticity, neurite extension, growth cone guidance, differentiation, and neuronal maturation, its downregulation results in neurite growth arrest, retraction, and abnormal morphology due to altered Ca<sup>2+</sup> signaling (Jurkovicova et al. 2007). Restored IP<sub>3</sub>R1 expression by ChABC did restore also neurite outgrowth. We suggest that while suppressed expression of IP<sub>3</sub>R1 is an important mechanism contributing to altered calcium signaling in a model of neuronal injury, contribution of VDCC is negligible.

Until now, ability of in vitro fibrotic scar model to mimic morphological (arrested neurite outgrowth) and molecular (expression of various molecules) changes in CNS injury was evaluated (Kimura-Kuroda et al. 2010; Shearer et al. 2003; Li et al. 2013; Carulli et al. 2005). Here, we have shown significant alterations of voltage-dependent sodium and potassium but not calcium currents in CGCs cultured on a fibrotic scar model. These changes may contribute to arrested neurite outgrowth and are fully ( $I_K$ ) or partly ( $I_{Na}$ ) reversible by ChABC. Observed changes cannot be reproduced by simple coculture of CGCs with TGF- $\beta$ 1 administration. Therefore, other factors then increased the expression of TGF- $\beta$ 1 in an injury site must contribute to altered cellular excitability.

**Acknowledgments** This work was supported by the Slovak Research and Development Agency under the contract No. APVV-0212-10.

**Authors Contribution** Katarína Ondáčová did the experiments, evaluated data, and participated in writing manuscript. Dana Jurkovičová designed and supervised experiments, and participated in writing manuscript. Eubica Lacinová designed and supervised experiments, participated in data evaluation, and participated in writing manuscript.

## Compliance with Ethical Standards

**Conflict of interest** Authors declare no conflict of interest and no financial interest in the publication of this manuscript

## References

- Amico C, Marchetti C, Nobile M, Usai C (1995) Pharmacological types of calcium channels and their modulation by baclofen in cerebellar granules. *J Neurosci* 15(4):2839–2848
- Anderson MA, Burda JE, Ren Y, Ao Y, O’Shea TM, Kawaguchi R, Coppola G, Khakh BS, Deming TJ, Sofroniew MV (2016) Astrocyte scar formation aids central nervous system axon regeneration. *Nature* 532(7598):195–200. doi:10.1038/nature17623
- Berry M, Maxwell WL, Logan A, Mathewson A, McConnell P, Ashhurst DE, Thomas GH (1983) Deposition of scar tissue in the central nervous system. *Acta Neurochir Suppl (Wien)* 32:31–53
- Brackenbury WJ, Calhoun JD, Chen C, Miyazaki H, Nukina N, Oyama F, Ranscht B, Isom LL (2010) Functional reciprocity between Na<sup>+</sup> channel Nav1.6 and beta1 subunits in the coordinated regulation of excitability and neurite outgrowth. *Proc Natl Acad Sci USA* 107(5):2283–2288. doi:10.1073/pnas.0909434107
- Cao Z, Cui Y, Busse E, Mehrotra S, Rainier JD, Murray TF (2014) Gambierol inhibition of voltage-gated potassium channels augments spontaneous Ca<sup>2+</sup> oscillations in cerebrocortical neurons. *J Pharmacol Exp Ther* 350(3):615–623. doi:10.1124/jpet.114.215319
- Carbonell AL, Boya J (1988) Ultrastructural study on meningeal regeneration and meningo-glia relationships after cerebral stab wound in the adult rat. *Brain Res* 439(1–2):337–344
- Carlier E, Dargent B, De Waard M, Couraud F (2000) Na(+) channel regulation by calmodulin kinase II in rat cerebellar granule cells. *Biochem Biophys Res Commun* 274(2):394–399. doi:10.1006/bbrc.2000.3145
- Carulli D, Laabs T, Geller HM, Fawcett JW (2005) Chondroitin sulfate proteoglycans in neural development and regeneration. *Curr Opin Neurobiol* 15(1):116–120. doi:10.1016/j.conb.2005.01.014
- Cull-Candy SG, Marshall CG, Ogden D (1989) Voltage-activated membrane currents in rat cerebellar granule neurones. *J Physiol* 414:179–199
- Davis TH, Chen C, Isom LL (2004) Sodium channel beta1 subunits promote neurite outgrowth in cerebellar granule neurons. *J Biol Chem* 279(49):51424–51432. doi:10.1074/jbc.M410830200
- Fawcett JW, Asher RA (1999) The glial scar and central nervous system repair. *Brain Res Bull* 49(6):377–391
- Fernandez-Klett F, Priller J (2014) The fibrotic scar in neurological disorders. *Brain Pathol* 24(4):404–413. doi:10.1111/bpa.12162
- George J, Dravid SM, Prakash A, Xie J, Peterson J, Jabba SV, Baden DG, Murray TF (2009) Sodium channel activation augments NMDA receptor function and promotes neurite outgrowth in immature cerebrocortical neurons. *J Neurosci* 29(10):3288–3301. doi:10.1523/JNEUROSCI.6104-08.2009
- Heath NC, Rizwan AP, Engbers JD, Anderson D, Zamponi GW, Turner RW (2014) The expression pattern of a Cav3-Kv4 complex differentially regulates spike output in cerebellar granule cells. *J Neurosci* 34(26):8800–8812. doi:10.1523/JNEUROSCI.0981-14.2014
- Ishikawa K, Tanaka M, Black JA, Waxman SG (1999) Changes in expression of voltage-gated potassium channels in dorsal root ganglion neurons following axotomy. *Muscle Nerve*

- 22(4):502–507. doi:[10.1002/\(Sici\)1097-4598\(199904\)22:4<502:Aid-Mus12>3.0.Co;2-K](https://doi.org/10.1002/(Sici)1097-4598(199904)22:4<502:Aid-Mus12>3.0.Co;2-K)
- Jabba SV, Prakash A, Dravid SM, Gerwick WH, Murray TF (2010) Antillatoxin, a novel lipopeptide, enhances neurite outgrowth in immature cerebrotal neurons through activation of voltage-gated sodium channels. *J Pharmacol Exp Ther* 332(3):698–709. doi:[10.1124/jpet.109.161802](https://doi.org/10.1124/jpet.109.161802)
- Jalonen T, Johansson S, Holopainen I, Oja SS, Arhem P (1990) Single-channel and whole-cell currents in rat cerebellar granule cells. *Brain Res* 535(1):33–38
- Jaskova K, Pavlovicova M, Jurkovicova D (2012) Calcium transporters and their role in the development of neuronal disease and neuronal damage. *Gen Physiol Biophys* 31(4):375–382. doi:[10.4149/gpb\\_2012\\_053](https://doi.org/10.4149/gpb_2012_053)
- Jaskova K, Pavlovicova M, Cagalinec M, Lacinova L, Jurkovicova D (2014) TGFβ1 downregulates neurite outgrowth, expression of Ca<sup>2+</sup> transporters, and mitochondrial dynamics of in vitro cerebellar granule cells. *NeuroReport* 25(5):340–346. doi:[10.1097/WNR.000000000000106](https://doi.org/10.1097/WNR.000000000000106)
- Jiao S, Liu Z, Ren WH, Ding Y, Zhang YQ, Zhang ZH, Mei YA (2007) cAMP/protein kinase A signalling pathway protects against neuronal apoptosis and is associated with modulation of Kv2.1 in cerebellar granule cells. *J Neurochem* 100(4):979–991. doi:[10.1111/j.1471-4159.2006.04261.x](https://doi.org/10.1111/j.1471-4159.2006.04261.x)
- Jurkovicova D, Kopacek J, Stefanik P, Kubovcakov L, Zahradnikova A Jr, Zahradnikova A, Pastorekova S, Krizanova O (2007) Hypoxia modulates gene expression of IP3 receptors in rodent cerebellum. *Pflugers Arch* 454(3):415–425. doi:[10.1007/s00424-007-0214-6](https://doi.org/10.1007/s00424-007-0214-6)
- Karmazinova M, Lacinova L (2010) Measurement of cellular excitability by whole cell patch clamp technique. *Physiol Res* 59(Suppl 1):S1–S7
- Kawano H, Kimura-Kuroda J, Komuta Y, Yoshioka N, Li HP, Kawamura K, Li Y, Raisman G (2012) Role of the lesion scar in the response to damage and repair of the central nervous system. *Cell Tissue Res* 349(1):169–180. doi:[10.1007/s00441-012-1336-5](https://doi.org/10.1007/s00441-012-1336-5)
- Kimura-Kuroda J, Teng X, Komuta Y, Yoshioka N, Sango K, Kawamura K, Raisman G, Kawano H (2010) An in vitro model of the inhibition of axon growth in the lesion scar formed after central nervous system injury. *Mol Cell Neurosci* 43(2):177–187. doi:[10.1016/j.mcn.2009.10.008](https://doi.org/10.1016/j.mcn.2009.10.008)
- Komuta Y, Teng X, Yanagisawa H, Sango K, Kawamura K, Kawano H (2010) Expression of transforming growth factor-beta receptors in meningeal fibroblasts of the injured mouse brain. *Cell Mol Neurobiol* 30(1):101–111. doi:[10.1007/s10571-009-9435-x](https://doi.org/10.1007/s10571-009-9435-x)
- Li HP, Homma A, Sango K, Kawamura K, Raisman G, Kawano H (2007) Regeneration of nigrostriatal dopaminergic axons by degradation of chondroitin sulfate is accompanied by elimination of the fibrotic scar and glia limitans in the lesion site. *J Neurosci Res* 85(3):536–547. doi:[10.1002/jnr.21141](https://doi.org/10.1002/jnr.21141)
- Li HP, Komuta Y, Kimura-Kuroda J, van Kuppevelt TH, Kawano H (2013) Roles of chondroitin sulfate and dermatan sulfate in the formation of a lesion scar and axonal regeneration after traumatic injury of the mouse brain. *J Neurotrauma* 30(5):413–425. doi:[10.1089/neu.2012.2513](https://doi.org/10.1089/neu.2012.2513)
- Logan A, Berry M, Gonzalez AM, Frautschy SA, Sporn MB, Baird A (1994) Effects of transforming growth factor beta 1 on scar production in the injured central nervous system of the rat. *Eur J Neurosci* 6(3):355–363
- Ma SH, Li B, Huang HW, Peng YP, Qiu YH (2012) Interleukin-6 inhibits L-type calcium channel activity of cultured cerebellar granule neurons. *J Physiol Sci* 62(5):385–392. doi:[10.1007/s12576-012-0215-x](https://doi.org/10.1007/s12576-012-0215-x)
- Mathie A, Clarke CE, Ranatunga KM, Veale EL (2003) What are the roles of the many different types of potassium channel expressed in cerebellar granule cells? *Cerebellum* 2(1):11–25. doi:[10.1080/14734220310015593](https://doi.org/10.1080/14734220310015593)
- Mattson MP (2007) Calcium and neurodegeneration. *Aging Cell* 6(3):337–350. doi:[10.1111/j.1474-9726.2007.00275.x](https://doi.org/10.1111/j.1474-9726.2007.00275.x)
- Moreira-Lobo DC, Cruz JS, Silva FR, Ribeiro FM, Kushmerick C, Oliveira FA (2016) Thiamine deficiency increases Ca current and Ca<sub>v</sub>1.2 L-type Ca channel levels in cerebellum granular neurons. *Cell Mol Neurobiol*. doi:[10.1007/s10571-016-0378-8](https://doi.org/10.1007/s10571-016-0378-8)
- Morgenstern DA, Asher RA, Fawcett JW (2002) Chondroitin sulphate proteoglycans in the CNS injury response. *Prog Brain Res* 137:313–332
- Murali SS, Napier IA, Mohammadi SA, Alewood PF, Lewis RJ, Christie MJ (2015) High-voltage-activated calcium current subtypes in mouse DRG neurons adapt in a subpopulation-specific manner after nerve injury. *J Neurophysiol* 113(5):1511–1519. doi:[10.1152/jn.00608.2014](https://doi.org/10.1152/jn.00608.2014)
- Nichols J, Perez R, Wu C, Adelson PD, Anderson T (2015) Traumatic brain injury induces rapid enhancement of cortical excitability in juvenile rats. *CNS Neurosci Ther* 21(2):193–203. doi:[10.1111/cns.12351](https://doi.org/10.1111/cns.12351)
- Rossi P, D'Angelo E, Magistretti J, Toselli M, Taglietti V (1994) Age-dependent expression of high-voltage activated calcium currents during cerebellar granule cell development in situ. *Pflugers Arch* 429(1):107–116
- Schaller KL, Caldwell JH (2003) Expression and distribution of voltage-gated sodium channels in the cerebellum. *Cerebellum* 2(1):2–9. doi:[10.1080/14734220309424](https://doi.org/10.1080/14734220309424)
- Shearer MC, Fawcett JW (2001) The astrocyte/meningeal cell interface—a barrier to successful nerve regeneration? *Cell Tissue Res* 305(2):267–273
- Shearer MC, Niclou SP, Brown D, Asher RA, Holtmaat AJ, Levine JM, Verhaagen J, Fawcett JW (2003) The astrocyte/meningeal cell interface is a barrier to neurite outgrowth which can be overcome by manipulation of inhibitory molecules or axonal signalling pathways. *Mol Cell Neurosci* 24(4):913–925
- Shibata R, Nakahira K, Shibasaki K, Wakazono Y, Imoto K, Ikenaka K (2000) A-type K<sup>+</sup> current mediated by the Kv4 channel regulates the generation of action potential in developing cerebellar granule cells. *J Neurosci* 20(11):4145–4155
- Stewart RR, Bossu JL, Muzet M, Dupont JL, Feltz A (1995) Voltage-activated ionic currents in differentiating rat cerebellar granule neurons cultured from the external germinal layer. *J Neurobiol* 28(4):419–432. doi:[10.1002/neu.480280403](https://doi.org/10.1002/neu.480280403)
- Struckhoff G (1995) Cocultures of meningeal and astrocytic cells—a model for the formation of the glial-limiting membrane. *Int J Dev Neurosci* 13(6):595–606
- Susarla BT, Laing ED, Yu P, Katagiri Y, Geller HM, Symes AJ (2011) Smad proteins differentially regulate transforming growth factor-beta-mediated induction of chondroitin sulfate proteoglycans. *J Neurochem* 119(4):868–878. doi:[10.1111/j.1471-4159.2011.07470.x](https://doi.org/10.1111/j.1471-4159.2011.07470.x)
- Toth AB, Shum AK, Prakriya M (2016) Regulation of neurogenesis by calcium signaling. *Cell Calcium* 59(2–3):124–134. doi:[10.1016/j.ceca.2016.02.011](https://doi.org/10.1016/j.ceca.2016.02.011)
- Viviani B, Gardoni F, Marinovich M (2007) Cytokines and neuronal ion channels in health and disease. *Int Rev Neurobiol* 82:247–263. doi:[10.1016/S0074-7742\(07\)82013-7](https://doi.org/10.1016/S0074-7742(07)82013-7)
- Wanner IB, Deik A, Torres M, Rosendahl A, Neary JT, Lemmon VP, Bixby JL (2008) A new in vitro model of the glial scar inhibits axon growth. *Glia* 56(15):1691–1709. doi:[10.1002/glia.20721](https://doi.org/10.1002/glia.20721)
- Zhuang JL, Wang CY, Zhou MH, Duan KZ, Mei YA (2012) TGF-beta 1 Enhances Kv2.1 potassium channel protein expression and promotes maturation of cerebellar granule neurons. *J Cell Physiol* 227(1):297–307. doi:[10.1002/jcp.22735](https://doi.org/10.1002/jcp.22735)